Journal homepage www.jzs.univsul.edu.iq
Journal of Zankoy Sulaimani
Part-A- (Pure and Applied Sciences)

Seismic Crustal and Upper Mantle Structure of Iraq and Surrounding Regions Inferred from Regional Waveform Inversions

Ghassan I. Aleqabi[1], Michael E. Wysession[1] & Hafidh A. A. Ghalib[2]

1 Washington University in Saint Louis, Campus Box 1169, One Brookings Drive, Saint Louis, MO 63130, USA, e-mail: ghassan@mantle.wustl.edu
2 Array Information Technology, 5130 Commercial Drive, Suite B, Melbourne, FL 32940, USA, e-mail: hafidh.ghalib@arrayinfotech.com

Article info

Original: 06.10.2015
Revised:02.05.2016
Accepted:19.05.2016
Published online: 15.06.2016

Key Words:
waveform matching
genetic algorithm
niching

Abstract

The shear wave (*S*-wave) velocity structure of the crust and its effect on seismic−wave propagation are of fundamental interest in many geophysical studies. *S*-wave velocities and layer thicknesses have a dominating influence on the waveforms of Rayleigh waves. Rayleigh wave waveforms from the Northern Iraq Seismographic Network (NISN) are inverted to constrain the crustal and upper mantle velocity structure in Iraq and surrounding regions. The inversion uses a niching genetic algorithm (NGA), which optimizes four parameters of earth properties at different frequencies and in different sub-populations: *P*-wave velocity, *S*-wave velocity, density, and Earth layer thicknesses. Each subpopulation separately performs the genetic algorithm processes of selection, crossover, and mutation of the velocity models, with the niching function removing models that are too similar to maintain distinct subpopulations. Using both observed earthquake surface waves waveforms and synthetic forward-modeled waveforms; we obtain regional S-wave profiles for the crust (including top-most sedimentary layers), and the upper mantle. We demonstrate that the NGA method is a robust means of interpreting observed surface-wave waveform data.

Introduction

Crustal structure plays a crucial role in studies of seismicity and other tectonic activity. Shortcomings in the knowledge of a region's crustal structure leads to serious inaccuracies in calculation of seismic event location, and event source characterization. It causes problems in analyzing wave propagation phenomena such as the travel time, amplitude, waveform shape, and the frequency content of regionally propagated phases. For those reasons, we intend to determine one- and two-dimensional crustal and upper mantle structures for the northern Arabian platform and surroundings plateaus using a niching genetic algorithm waveform inversion method. This technique is applied to regional waveforms traversing the Turkish-Iranian Plateau and the Arabian plate. The Niching Genetic Algorithm (NGA), as implemented in this study, performs a search of a predefined model parameter space to infer crustal and upper mantle structures. NGAs provide alternative solutions (models) that are valuable for statistical analysis as well as their uncertainty values. Results of this study will include one- and two-dimensional models for paths within the region. Statistical analyzes of the final models provide estimates of uncertainties in the inverted parameters (layer thickness, shear wave velocity, and attenuation). In this study, we independently assess the adequacy of the

inferred structures in predicting travel times of regional phases and in expressing waveforms and their dispersion parameters. Knowledge of crustal and upper mantle structures and their associated uncertainties will provide a means of updating current velocity models and will improve our understanding of the tectonic history of the region.

Seismic waveforms of regional earthquakes have been collected over the last ten years from the Northern Iraq Seismographic Network (NISN). The NISN is a network of 10 broadband sensors with a unique location on the regional tectonics framework of the area *[1]*. We intend to address significant areas of uncertainty that may contribute to the observed discrepancies in analyzing the travel time, shape, amplitude, and frequency content of regional phases where the crustal and upper mantle structure are unconstrained. We will characterize one- and two-dimensional models of the structures (shear velocity, thickness, and attenuation) of the crust and upper mantle of the northern Arabian Peninsula (Iraq and Syria), Iran, Turkey, and Arabian plate using a regional waveform and travel time inversion method that employs the niching genetic algorithm. This technique performs a search of the model space and an examination of alternative local minima. In this study we address the following objectives using the NISN deployment data:

1. What is the crustal and upper mantle structure of the Northern Arabian Plate and surrounding regions? Can we successfully find viable regional structures that explain regional phases?
2. Is the crust significantly thickened in the Plateaus to accommodate the collision between the Arabian and Eurasian plates?

Regional earthquakes occurring within the Arabian plate and the Iranian and Turkish Plateaus provide significant ray paths coverage of Iran, Syria, Iraq, and Turkey as seismic waves propagate toward NISN stations (*Figure: 1*).

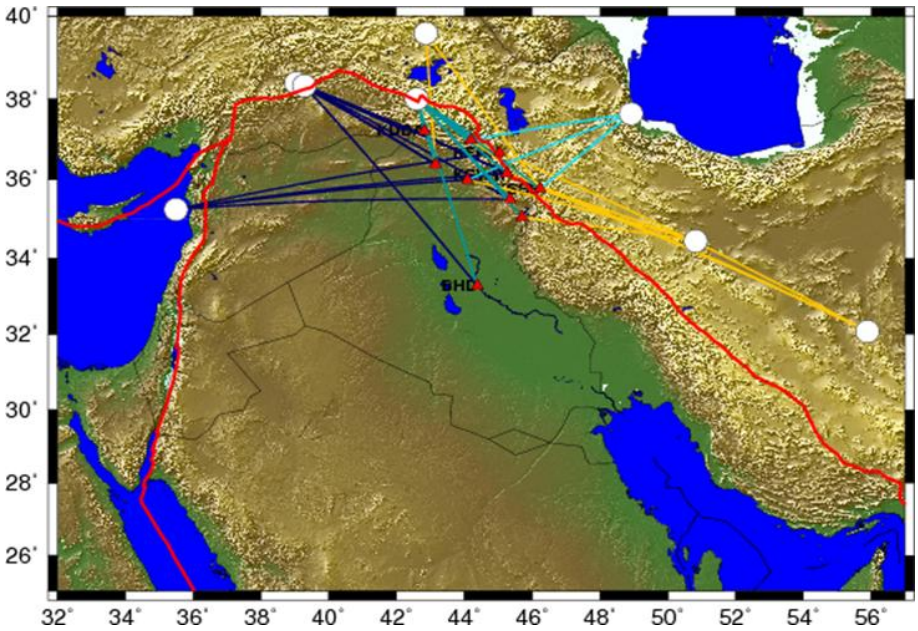

Figure-1: Map showing the geographic locations of the 10 broadband seismic stations (red triangles). White circles are locations of sample events that have their event-paths (colored lines) sampling the various tectonic environments in and around the Northern Iraq Seismic Network (NISN).

These unique event-station paths will allow a thorough characterization of the crustal and upper mantle structure of this region. Dispersed waveforms from Love and Rayleigh waves as well as travel times of first-arriving body waves will be used to characterize shear-wave velocities in the area by using a niching genetic algorithm. *Figure: 2* shows an example of an event with the pronounced definition of regional body and surface wave phases observed at station KEHH. This event located in western Syria and its wave train traversed the Northern Arabian Platform. Regional one- and two-dimensional velocity models developed

during this research will evaluate for accuracy through error bounds.

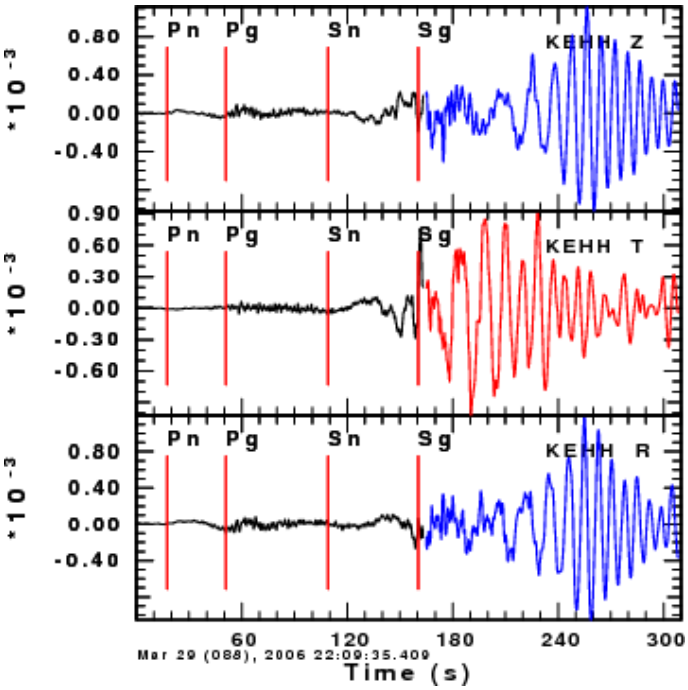

Figure-2: An example of a 3-component record of a regional earthquake from western Syria (20 March 2006) recorded at station KEHH of the NISN. The broadband waveforms show body waves (black) in addition to well-dispersed Rayleigh fundamental modes (blue) and Love fundamental modes (red).

Tectonic Setting

The Arabian Plate and the neighboring Iranian and Anatolian Plateaus have very complex and unique tectonic settings that have undergone changes in recent geologic time. The geologic structure of this region is dominated by the collision and suturing of the Arabian plate with the Eurasian plate and the formation of the Turkish-Iranian Plateau. The northeast-moving Arabian plate and the accompanying westward escaping of the Anatolian block currently control the tectonics along this suture.

During the Late Miocene suturing, intraplate volcanism continued in the eastern Anatolia. The tectonic convergence resulted in the westward movement of the Anatolian block (crystalline massifs of exhumed orogenic middle crust) between two major strike-slip zones, the northern and eastern Anatolian faults. The collision resulted in the uplift of the Eastern Anatolian Plateau (EAP) and the formation of the Bitlis-Zagros mountain belt. The Bitlis-Zagros belt wraps around the northern Arabian platform running from the NE-SW trend along the Eastern Anatolian Fault zone to an NW-SE trend along western Iran. The Bitlis-Zagros suture forms a seismically active linear belt extending from eastern Turkey to the Strait of Hormuz. The southwestern foothills of this belt form the northeastern fold and thrust zone of Iraq. West of the Zagros fold and thrust belt is the Mesopotamian Foredeep, a great basin of sediments stretching from Baghdad to Kuwait along the border of Iraq-Iran. West of the Mesopotamian Foredeep region, an interior stable platform (west of the Tigris River) stretches from the Syrian border to the Saudi Arabian border.

Seismic Waveform Inversion

The NGA waveform inversion is a non-linear waveform-fitting procedure that aims at obtaining estimates of an earth-structure velocity model from observed seismic waveforms. First, synthetic seismograms are computed as predicted data, using a given initial set of velocity models. Those models are then genetically processed to reduce the misfit between the observed and predicted data. This procedure is repeated iteratively, for successive generations of synthetic seismograms until the misfit between the predicted and observed sufficiently small.

1. Forward Problem and Velocity Model Parameterization

The forward problem involves calculating the synthetic seismograms of surface waves. The authors calculate first mode synthetic seismograms for Rayleigh and Love wave using a mode summation method *[2, 3, 4]*. Synthetic Green's functions were convolved with a parabolic source-time function having a base of $4l/dt$ time points, where l is the duration and dt is the time increment between samples. The mode-summation technique was chosen for calculating synthetic seismograms in order avoid the extensive synthetic seismogram calculation involved in the wavenumber integration technique, keeping in mind that we are interested in generating synthetic seismograms only for the fundamental-mode surface waves and in calculating arrival times of body waves.

The velocity models considered to the waveform inversion implemented in this study, to be a laterally homogeneous layered structure, with three unknowns. The inversion solves for the layers' thicknesses, and for the shear wave velocities, and attenuation quality factor (Q) values in each layer, and it calculates body wave travel times. Shear-wave velocities are sought in the inversion because Love and Rayleigh's waves dominate regional seismograms, and both are sensitive to the model's shear velocities. We adopted a 5- and 6-layer velocity structure. The layers are a sedimentary surface layer, and crustal layers, an uppermost mantle, and a half-space. To ensure that the shear wave velocity increases with depth, the first layer in the model acquires its velocity randomly from predefined lower and upper-velocity limits on the allowed values of the velocity. In the subsequent layers, beneath the first layer the velocity value is derived by randomly choosing velocity increment from a provided range of values for that layer (*i.e.*, each layer has its velocity range from which a velocity increment is randomly chosen) and adding it to the velocity value of the layer above it. This process is repeated for subsequent layers. The half-space will assign the same velocity and Q values as those of the bottom layer. This technique allows for the random selection of velocity values at each layer and ensuring that the shear-wave velocity increases with depth (*i.e.*, no low-velocity layers are allowed).

The compressional velocity structure is derived from the shear-wave velocity values using a ratio of 1.732 between the P and S velocities and assuming Poisson medium. Layer thicknesses, as well as the Q value for each layer, are randomly chosen from the user-defined search ranges for each layer in the model. This method requires no prior information on the structure and performs a thorough search of the model space. The details of the genetic algorithm will present in the ensuing sections. The main idea of this method is to test a large number of randomly generated model realizations and to select the one with the lowest minimum of the measure of the misfit between predicted and observed data. The result of the inversion process is a single best-fitting model within an ensemble of models.

2. Niching Genetic Algorithm

The Genetic Algorithms (GA) belong to a class of randomized search algorithms that are based on biological evolution. This analogy to biological evolution involves aspects of reproduction, genetic mutation, and natural selection, which are processes that allow us to use the GA in solving geophysical inverse problems. For example, a group of randomly generated velocity models computed with parameter values that fall within user-set limits can be examined through a GA to find an optimum velocity model. For each velocity model, the forward problem is solved, and a fitness value is assigned, based on a suitable reproductive function (objective function). The objective function is constructed as a $L2$ norm of the time-domain difference between the synthetic and observed seismograms. Mathematically, the difference (misfit) between the synthetic signal S at r_1 and the observed signal s at r_1, is a function of the velocity model, β, and it is mathematically expressed as

$$F(\beta) = \sum_1^N \int_0^T |S(t, r_1, \beta) - s(t, r_1)| \; dt \tag{1}$$

where $F(\beta)$ is the objective function, β is the model (shear-velocity, layer thickness and attenuation structure as a function of depth), T is the time window, and N is the number of recording stations. The vector β (i.e., the model) that minimizes the function $F(\beta)$ is considered a solution to this problem.

The objective function value (cost/misfit/penalty/fitness) is constructed from the sum of the individual misfits originating from the radial, transverse, and vertical components including body wave travel time residuals. The misfit values thus obtained will then decide the fate of each given model, which is either eliminated from the population or allowed to "breed" and transfer its traits to the next generation. After breeding, a crossover function is activated, and the models are subjected to random mutation. The genetic algorithm continues throughout a user-defined number of generations, converging on a solution that produces the least error if the parameters are set correctly *[5, 6]*. While the genetic algorithm converges to multiple solutions with local error minima, it does not guarantee that the best solution attains the global minimum. A suggested approach is, therefore, to run parallel genetic algorithms on several competing subpopulations

(models) to avoid premature convergence to a local minimum. In an implementation of this scenario, several subpopulations (demes) pursue a niche in the model space; thus, the term niching genetic algorithm (NGA) is applied to the method *[5, 7, 8, 9, 10]*. In summary, the NGA is similar to the genetic algorithm in the ways that it utilizes analogs of natural selection processes, but it has an extra step, in which it promotes the best solutions in each subpopulation (demes) that form the generation population. In this promotion process, the best solutions in each subpopulation are made to be different since there will be a penalty function assigned that causes similar best members between the subpopulations to be purged. This will force subpopulations diversity and promotes subpopulations, causing to explore regions of the model space, searching for the global minimum rather than individual members (velocity models) from the subpopulations converging to a small region within the model space.

Finding an earth model that explains details in the observed wavefield is a challenging problem, and the NGA are a suitable technique to solve it *[10, 11]*. The niching genetic algorithm method can summarize in the following specific steps:

1) Define the number of generations.
2) For each generation, initialize n members of the sub-populations (demes) to form a generation. Each deme has k members consisting of velocity models *vm* and

$$V_{nk} = \begin{bmatrix} (vm_{01}, vm_{02}, \dots, vm_{0k}), (vm_{11}, vm_{12}, \dots \dots, vm_{1k}), \\ (\dots \dots), (vm_{n1}, vm_{n2}, \dots, vm_{nk}) \end{bmatrix}$$

3) Solve the forward problem to obtain synthetic seismograms using velocity models in #2.
4) For each model, a fitness value is calculated by finding the difference between the synthetic seismograms (calculated in #3) and the observed waveforms using equation (1).
5) The GA will pair the velocity models vm to form the new vm pairs of the new generation.
6) With a certain crossover probability, the crossover operator acts on the selected pairs (step 5) to produce new pairs of vm.
7) With a certain mutation probability, the mutation operator is applied to each member.
8) Use the resulting vm from the sub-populations to assemble the new generation.
9) Repeat steps 3 to 8 for the predefined number of generations in 1.

Members of the first *deme*, $(n = 1)$ will continue to the next generation as a regular GA, while the best member of $(n > 1)$ demes are compared to the best models from the other demes for similarity. For the models with similarity metrics greater than a predefined value of the critical radius of separation, R_c (the measure to which a solution will be penalized for similarity to the solutions in other demes) will have their cost replaced by the cost of the worst model (high cost), effectively weeding it out by the GA selection operator. The process of eliminating elite models from the demes on the basis of their similarity will continue for $(n - 1)$ times. The R_c value is critical to the nature of the NGA inversion. A too-small value will allow each model to converge to a different minimum; a too-high value of R_c will allow subpopulations to be similar to the first subpopulation and their ability to explore separate portions of the model space is therefore curtailed. A moderate value will allow demes to thoroughly explore the model space and converge to local minima with sufficient distance from the global minimum. The NGA will produce *n* viable solutions (the number of demes assigned), from which a global minimum will be determined. Those solutions have the lowest cost and can be evaluated in terms of their ability to explain the observed seismograms and travel times of body waves and the visual comparison between the observed and the theoretical dispersion curves that are computed for the final velocity models.

3. Waveforms Paths and Signals Preparation

The geographical location of NISN in the northeast of the Arabian platform allows its equipment to record regional seismic events from the surrounding seimic sources. For calculating the forward problem, the earthquakes' locations and source mechanisms are required. Earthquake locations are taken the Preliminary

Determinations of Epicenters (PDE) bulletin [http://earthquake.usgs.gov], and the mechanisms of origin are taken from the Global Centroid-Moment-Tensor (CMT) bulletin at [http://www.globalcmt.org. The inversion method used has no limitation on the frequency content of the inverted surface wave window, but some filtering is required to weed out scattered and multi-path waves. The waveforms' preparation for the inversion involves removing the instrument response, rotating the horizontal components to the radial and transverse directions. This is followed by, generating Phase-Match-Filtered (PMF) seismograms of the fundamental mode Rayleigh or Love surface wave *[12, 13, 14]*. In the inversion, the extracted PMF waveforms are preferable to the original waveforms because they have reduced noise and body wave signals. A time window appropriate for the epicentral distance is defined to isolate the surface-wave energy used in the inversion.

Application to NISN

1. One-Dimensional Velocity Structures

The NGA joint waveform inversion method is applied to a suitable seismic data set from NISN and for paths sampling tectonic regions of the area (*Figure: 1*). The ability to invert waveforms using NGA from regional events is tested with an event located in central Iran (*Figure: 3*). The event occurred on 7 April 2007. It has a focal depth of 12 km, $m_b = 4.7$, and an epicentral distance to the NISN station KSSS (32.2°N, 55.9°E) of 982 km. Surface-wave energy from this event sampled the Iranian Plateau.

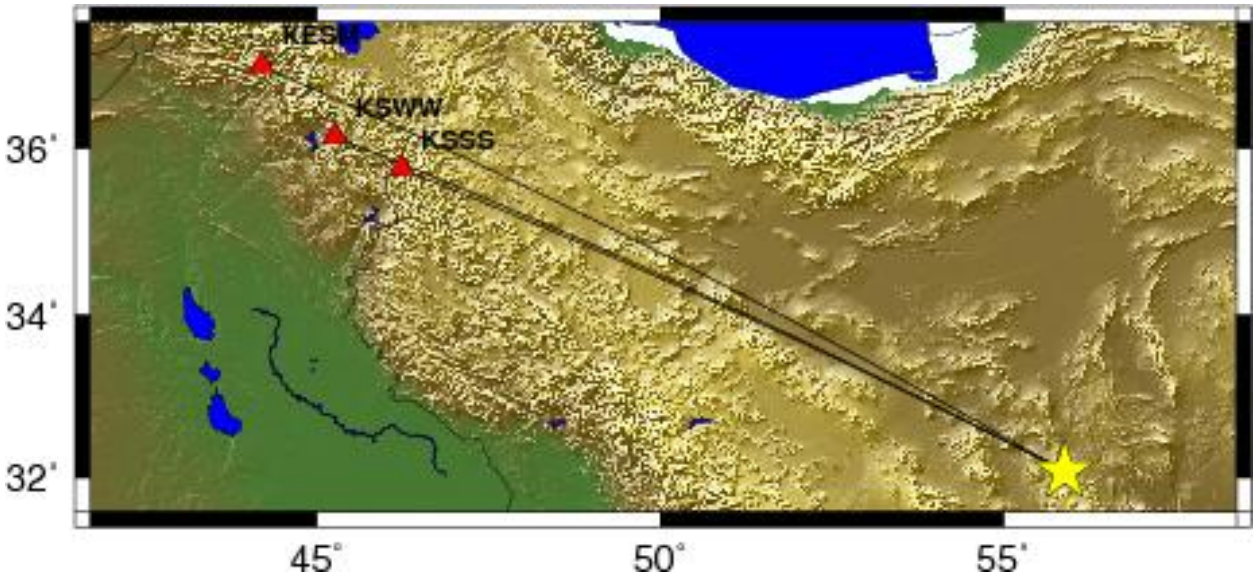

Figure-3: The map shows the location of the chosen earthquake in central Iran (yellow star) and the ray paths traversed through the Iranian Plateau (black lines) to NISN stations KESM, KSWW, and KSSS in northern Iraq (red triangles).

We computed synthetic seismograms for this event using a velocity model for the Iranian Plateau from *[15]*, shown in *Figure: 4*. It shows P-wave profile (right panel) and S-wave velocity models (right panel). The left panel in Fig. 4 depicts two P-wave velocity profiles. The blue line shows the velocity profile for the Iranian Plateau *[15]*, and the red line displays the velocity profile obtained from NGA inversion along the path between central Iran and the NISN station KSSS. The right panel of *Figure: 4* shows two S-wave velocity profiles. The blue line is for the Iranian Plateau from *[15]*, and the red line is the S-wave velocity from NGA waveform inversion along the same path between central Iran and station KSSS.

The comparison of observed waveforms from the central Iran event with the synthetic seismograms computed using the velocity model from *[15]* is shown in *Figure: 5*. We notice significant discrepancies between observed surface waves and synthetic surface waves at KSSS, especially for the vertical and radial components. The velocity model from *[15]* is limited in expressing regional waveform shapes and arrivals because it was created from an insufficient number of good regional seismic waveforms. *Figure: 6* shows the

improved comparison of the data seismograms with synthetic seismograms computed using our NGA waveform inversion method. This example illustrates the advantage of using the NGA waveform inversion in providing a means of constraining velocity structure. The velocity models adopted in this inversion have six layers and a half space. The NGA included 5 demes, each which 36 velocity models, for a total of 180 models that were evaluated in each generation, and, therefore, a total of 27000 models were evaluated for an inversion running for 150 generations.

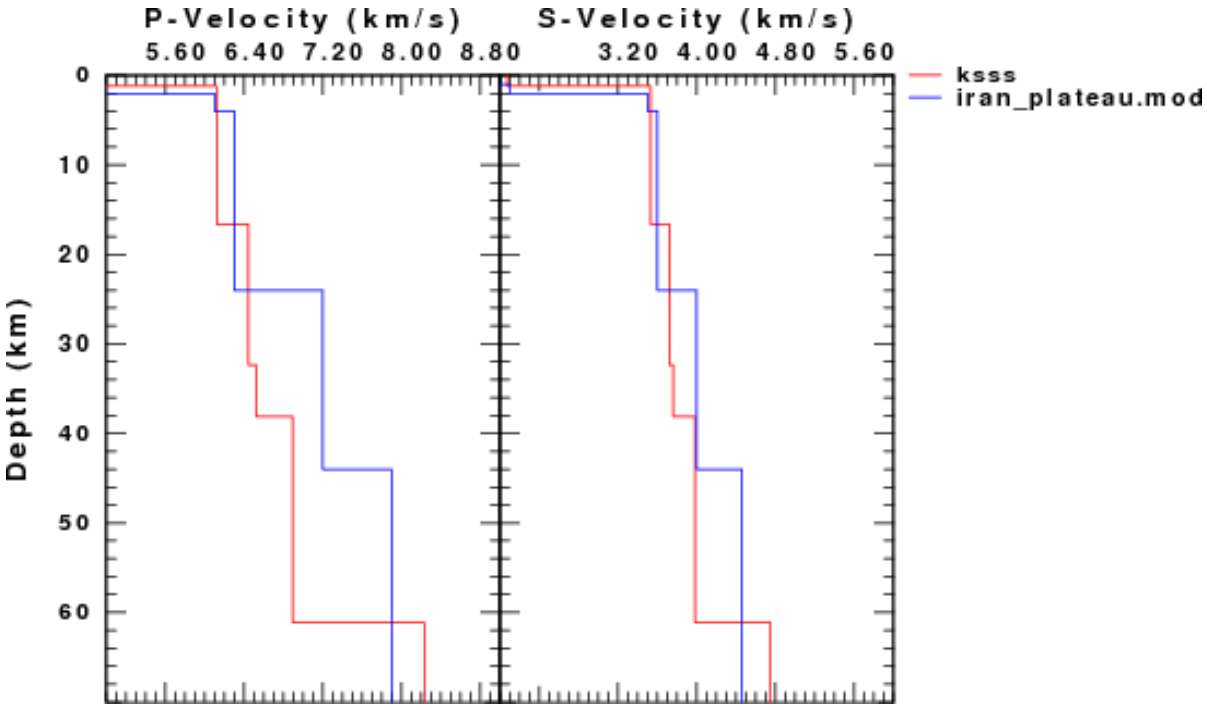

Figure-4: P-wave (left panel) and S-wave (right panel) velocity profiles for two different earth models. The blue lines show the P and S velocity profiles for the Iranian Plateau *[15]*, and the red lines show the profiles obtained from NGA waveform inversion along the path between central Iran and station KSSS.

Figure-5: Waveform fit between observed surface waves (Rayleigh = Blue; Love = red) on the radial, transverse and vertical components from a central Iran event, along with similar components from synthetic seismograms (black) calculated using the Iranian Plateau velocity model of *[15]*, show in *Figure: 4*.

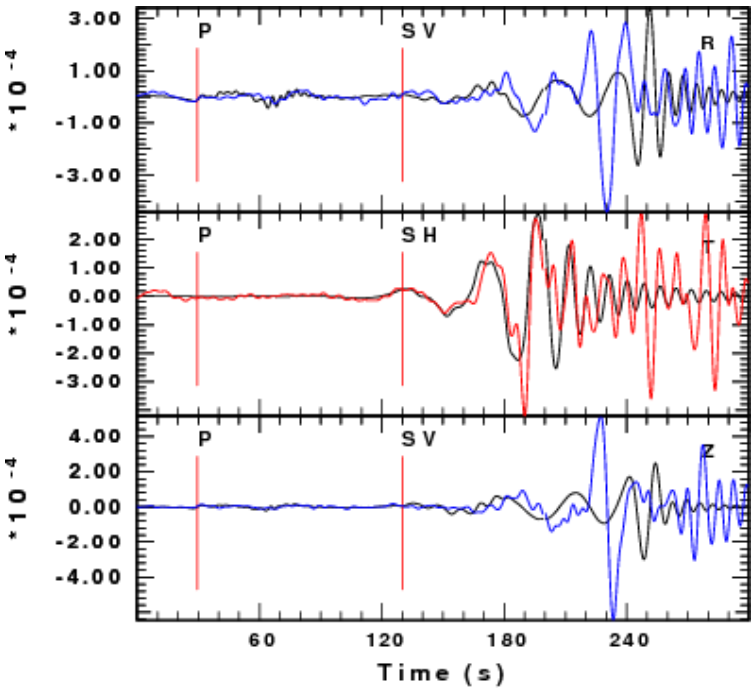

The authors simultaneously inverted the observed Love and Rayleigh surface wave waveforms and the arrival times of the first-observed P- waves. The two velocity models are shown in *Figure: 4* are evaluated

regarding their ability to reproduce observed waveforms. We found the NGA inversion produced a model that is viable and can explain the main characteristics of the observed waveforms with a greater degree of resemblance than the model provided by *[15]*. The NGA method provided a final velocity model that produced an excellent fit between observed and synthetic signals (*Figure: 6*). This model is also used for comparing theoretical dispersion values with the observed dispersion values. *Figure 7* shows this comparison, where the calculated dispersion curves match the observed dispersion. This independent test shows that a well-parameterized NGA inversion method for regional waveforms offers a new means to find effectively unique velocity models.

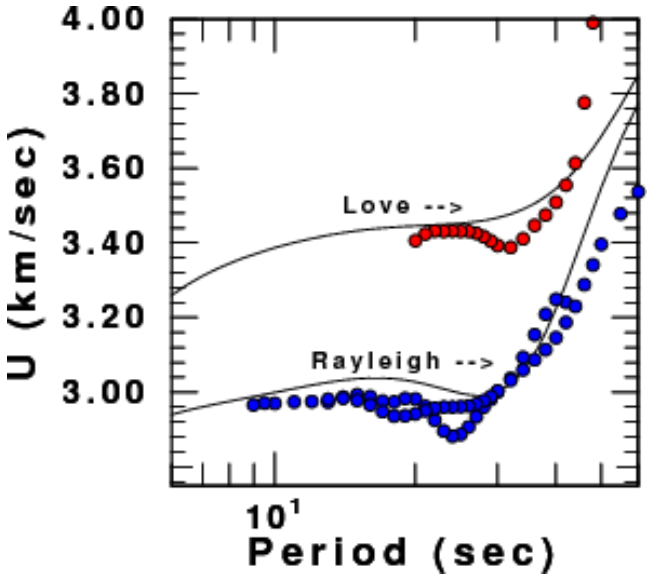

Figure-6: Waveform fit between observed surface waves (Rayleigh = blue; Love = red) on the radial, transverse and vertical components from the central Iran event, along with similar components from synthetic seismograms (black) calculated using the Iranian Plateau velocity model calculated from the NGA waveform inversion technique (*Figure: 4*). The wavenumber integration technique was used to compute the synthetic seismograms. The match between observed and synthetic seismograms is significantly improved, indicating that it is possible to characterize the crustal and upper mantle structure for the Iranian Plateau using the path between the central Iran event and the NISN seismic station KSSS.

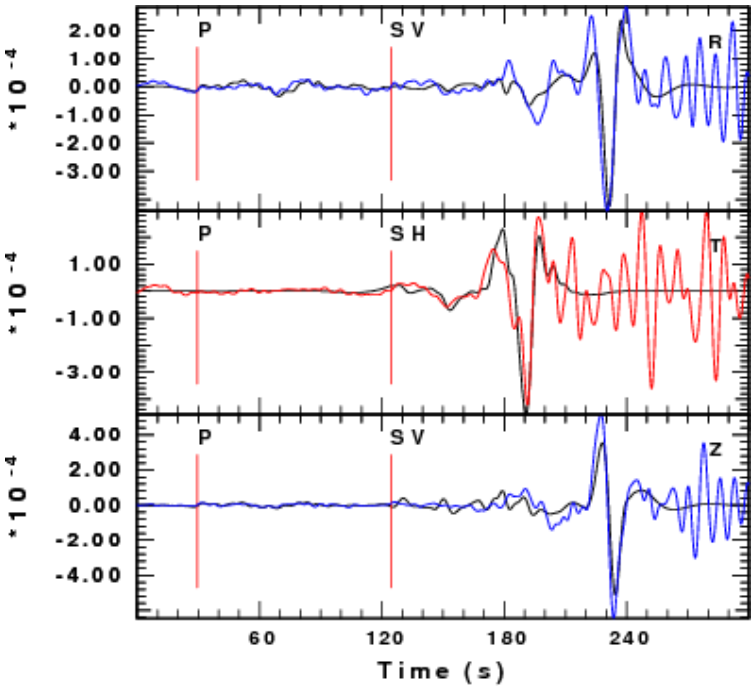

Figure-7: Observed Rayleigh (blue dot) and Love (red dot) wave fundamental mode group velocity dispersion values found from using phase match filtering. Those values are compared to Love and Rayleigh (black lines) theoretical dispersion curves calculated from the best velocity (*Figure: 4*, red lines) model obtained from the NGA inversion for the central Iran path to station KSSS.

2. Two-Dimensional Velocity Structure

In this section, we shall focus on modeling surface waves moveouts caused by lateral changes in the crust and upper mantle. For certain combinations of events and-stations, the geometry forms a pseudo-linear array. This linear arrangement provides a geometry that can be used to study lateral variations in the crust and upper mantle by modeling surface-wave moveouts. The proposed technique is to evolve (propagate) an observed surface-wave wavefield outward from the recording site to a suite of other stations and compare the

propagated wavefields with the observed data that were recorded there. This technique requires velocity models to provide dispersion parameters by which the observed wavefield phase will be perturbed to produce the required time shift (the shift of the propagated waveform that best matches the observed waveform). These velocity models will be constrained by using an NGA waveform inversion similar to what was described in seismic waveform inversion section, but with modifications to allow for a two-dimensional structure. In this technique, the recorded signal is assumed to consist of a single mode, namely a fundamental-mode Rayleigh or Love wave. Mathematically, numerical propagation can be summarized as follows: A frequency-domain perturbation of the signal phase terms by dispersion parameters cause a time shift in the time domain. The observed signal at distance r and frequency f is $S(r,f)$. With $k(f)$ as the wave number and $\gamma(f)$ as the anelastic attenuation, the expected signal at distance a r_1 is

$$S(r_1,f) = S(r,f)\left(\frac{r}{r_1}\right)^{1/2} e^{-\gamma(r_1-r)} e^{-ik(r_1-r)} \quad (2)$$

If the predicted time series at distance r_1 does not match the observed surface-wave energy at r_1, then the variation in the waveform represents a variation in earth structure. This formula provides a straightforward operator by which any recorded dispersed signal at a station could be propagated to a given distance if dispersion parameters (phase velocity, group velocity, and attenuation coefficients) of the velocity structure along the propagation path between the station and the subsequent suite of stations are provided. This concept is the basis of numerically propagating a dispersed signal outward using path-dispersion parameters and comparing the propagated signal to the observed signal at subsequent stations. We shall implement the NGA waveform inversion technique to constraint the inter-station models that form a two-dimensional laterally varying structure along the path. Model parameterizations are similar to the one-dimensional case described in seismic waveform inversion section, and for each linear path with more than one station, we need more than one model (segment) to parameterize the structure along the array. The number of segments between stations, plus one additional segment for the event to the first station determine the required number of models. The segment is a 1-D velocity model to represent the velocity model between two consecutive stations. An example showing how this technique is performed uses waveforms from an event located in the Anatolian Plateau (*Figure: 8*) (PDE parameters: 2007/02/09 02:22:55, 38.39°N, 39.04°E). Stations KDDA, KSWW, and KSSS of NISN are all within a 4° sector in back-azimuth from the event and they therefore form a mini-linear array with this event.

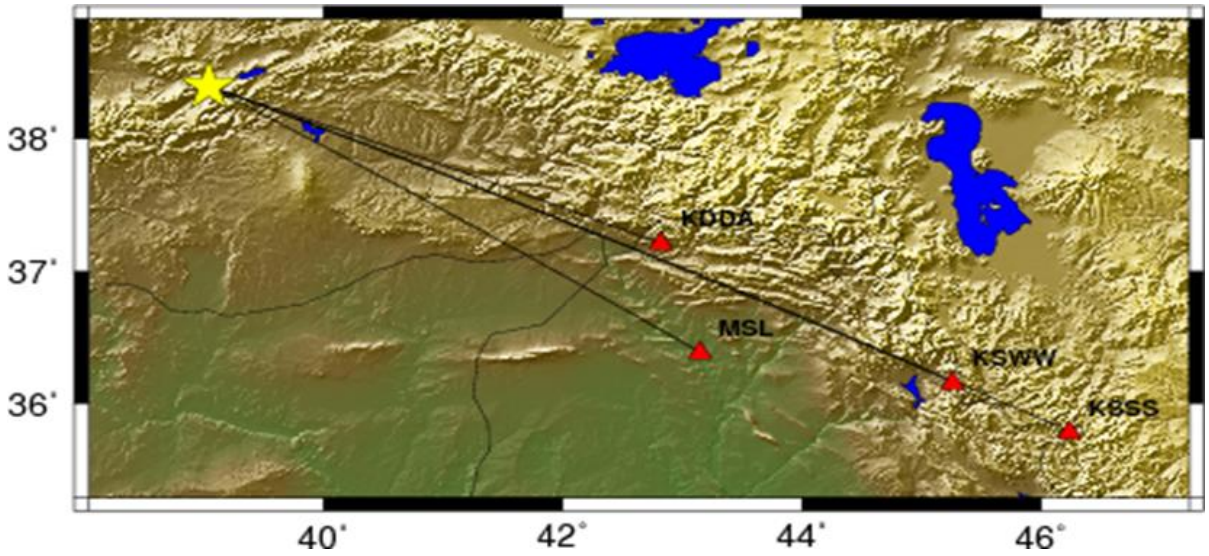

Figure-8: Map of northern Arabian platform and surroundings regions. The earthquake location is shown as a yellow star and the NISN stations KDDA, KSWW, and KSSS are shown as red triangles. We see that these stations and the event form a small array along which the waves traversed through the northern Arabian platform and Zagros Mountains.

Figure: 9 shows a record section of the PMF vertical component waveforms (black lines) recorded at the three stations KDDA, KSWW, and KSSS. The isolated signal at station KDDA will be propagated to the subsequent stations KSWW and KSSS using equation (2), and the propagated signals will then be compared to the signals observed at stations KSWW and KSSS.

To demonstrate the value of arriving at a two-dimensional structure by using the NGA waveform inversion, we tested the technique by propagating the PMF waveforms at KDDA and KSWW to station KSSS using a one-dimensional velocity model. This model was obtained from the NGA waveform inversion for the source-receiver path between the event located in Turkey and station KSSS using the technique described in seismic waveform inversion section. *Figure: 9* shows the comparison of waveforms. We notice significant discrepancies between the propagated and observed surface-waves at KSWW and KSSS. We concluded that a one-dimensional velocity model could not produce propagated waveforms that would match observed wave fields at KSWW and KSSS.

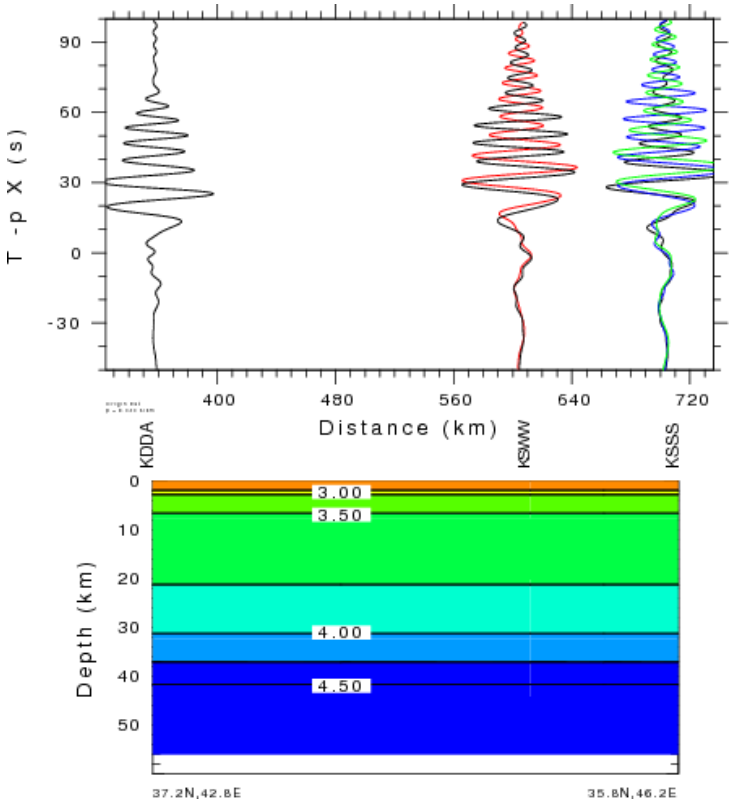

Figure-9: (top) Record section of observed phase-matched vertical-component fundamental-mode Rayleigh waves (black) and their congruent fundamental-mode Rayleigh wave waveforms (red, green, and blue) numerically propagated through the inferred 1-D model. (bottom). The model was obtained from fitting the waveforms at station KSSS from event 2007:040. Seismograms are plotted with a reduction velocity of 3.0 km/sec. From this example, the authors notice that there is a mismatch between the observed and propagated seismograms. It is evident that the model is inadequate to explain the observed waveforms' shapes and arrival times, and a 2-D model is needed instead.

Therefore, to improve the fit and eliminate discrepancies between the propagated and observed waveforms, we sought to invert for a two-dimensional velocity profile, where velocity changes both laterally and vertically. A profile (cross-section) is constructed from the constrained 1-D velocity models (segments) to represent a laterally varying velocity structure between stations KDDA and KSWW and between stations KSWW and KSSS. For the NGA 2-D waveform inversion, we assumed two adjacent structures and solved for their layer thickness, shear wave velocity, and attenuation structure. Each structure represents a segment of the propagation path. One segment is for KDDA-KSWW, and the other is for KSWW-KSSS.

Figure: 10 illustrates the advantage of using the 2-D inversion method. In using 2-D model, the mismatch in waveforms is totally eliminated and a more realistic velocity profile is found along the propagation path. The velocity profile is tested along the KDDA-KSSS path by propagating the observed signal at KDDA through the velocity model of segment KDDA-KSWW, and the observed signal at KSWW as well as the signal propagated the signal to KSWW from KDDA are then both propagated through the second segment between KSWW and KSSS. In this example, we have demonstrated that this method provides a means for solving the inversion problem for 2-D velocity structure. The excellent match (*Figure: 10*) indicates that we

can model the 2-D structure beneath the small array KDDA-KSSS. The KDDA-KSWW segment is within the Northern Arabian platform, and so its velocity is faster than that of the KSWW-KSSS segment, which is within the Zagros Mountains.

The propagated signal pair was cross-correlated to determine the inter-station phase velocity between stations KDDA-KSWW (*Figure: 11*, red circles). Similarly, the propagated signal pair that arrived at KSWW and KSSS was cross- correlated to determine the inter-station phase velocity between the stations (*Figure: 11*, blue circles). Individual inter-station phase velocity measurements (red and blue circles in *Figure: 11*) are compared to the theoretical phase velocities calculated for each model of the two segments that formed the laterally varying model (result of the inversion) and with the average 1-D model between the event and KSSS (thin black lines in *Figure: 11*). The good fit (*Figure: 11*) between the theoretically calculated phase-velocity values and observed phase velocity measurements inferred from the cross correlations of propagated signals provides another degree of confidence in the NGA models.

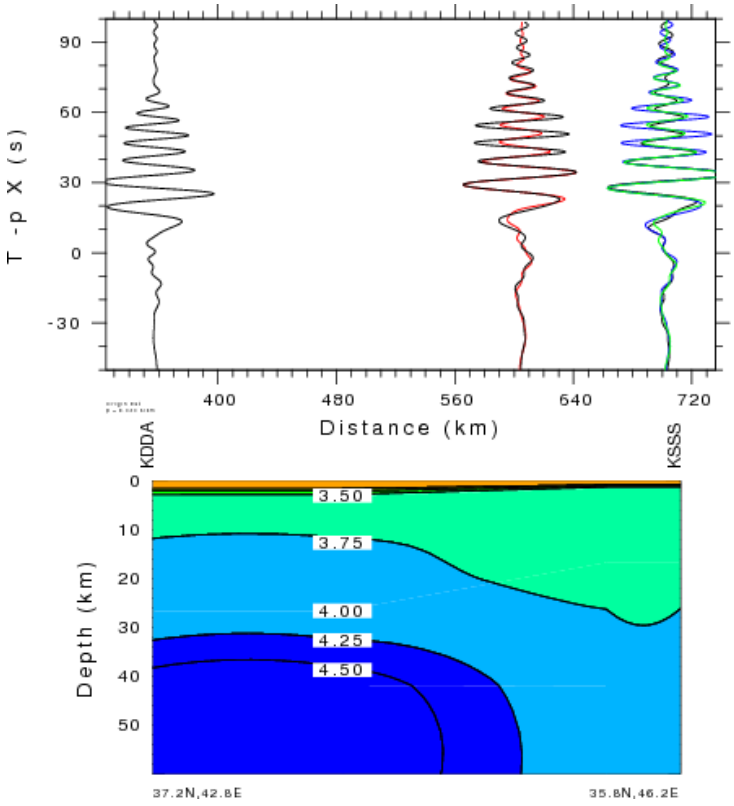

Figure-10: (top) Record section of observed phase-matched vertical-component fundamental-mode Rayleigh waves (black) from event 2007:040 plotted with a reduction velocity equal of 3.0 km/sec, shows with the congruent fundamental-mode Rayleigh wave waveforms (red, green, and blue) propagated through the inferred 2-D shear wave velocity profile (bottom). An excellent match for waveform is depicted between the observed and propagated signals.

Sources of Error, Uncertainty, and Model Resolution

We use phase-match filtering to isolate the fundamental mode surface waves from other signals. The error arises from the assumption that the isolated signal contains the only energy of the fundamental mode. Probably, other wave types are still present. Errors can also be introduced by differences in propagation paths and from biases during processing and inversion. The GA method is a nonlinear method, which limits our ability to obtain formal resolution and error estimates on the solutions. Statistical analyzes of the solutions (velocity models) from the demes will allow error estimations since those models have survived through generations, and they must have therefore posses qualities that are similar to the optimal solution.

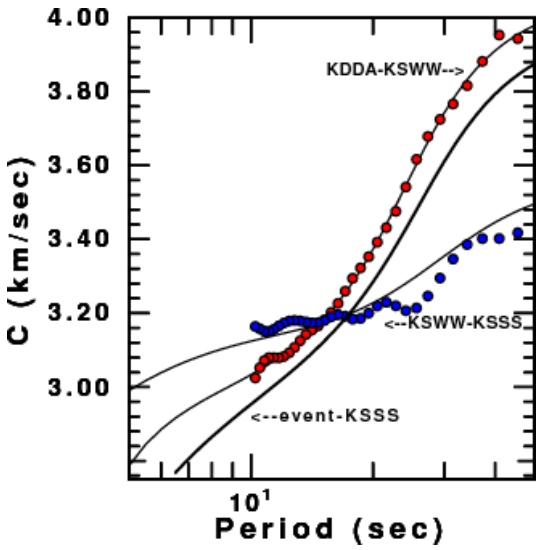

Figure-11: Comparison of observed Rayleigh wave fundamental mode phase velocity dispersion values (blue and red circles) extracted using a cross-correlation of propagated signals with the theoretical phase-velocity values of the two-segment model (black lines). The phase velocity dispersion curve (thick black line) of the average structure obtained by the NGA inversion of waveforms at KSSS from 2007:040 event is also depicted for comparison. We notice that this curve resembles the KDDA-KSWW curve in shape. This is expected, as the segment KDDA-KSWW represents 70% of the total path from the event to KSSS and it has lower phase velocities than both models for periods less than 18s and intermediate phase velocities between the two models for periods greater than 18s.

We consider the last generation solutions to have the best models of each subpopulation, and, therefore, variations within those models on the best model provide error bounds on the resultant optimal model of the generation. For each segment, we calculated the standard deviations of the shear wave velocity and thickness of each layer from the one-dimensional velocity models of the last generation, thus *Figure: 12* provides a summary comparison of the velocity models for each segment of the propagation path KDDA-KSSS. We found that the variations were increased with the depth and extent of the propagation path, with more variations along the segment KDDA-KSWW, which forms 70% of the entire paths, then along the segment KSWW-KSSS. This is expected, as wave propagation over longer path will encounter more lateral variations than the shorter path of propagation. A map of the standard deviation of the shear wave velocities along the KDDD-KSSS profile is presented in *Figure: 13*.

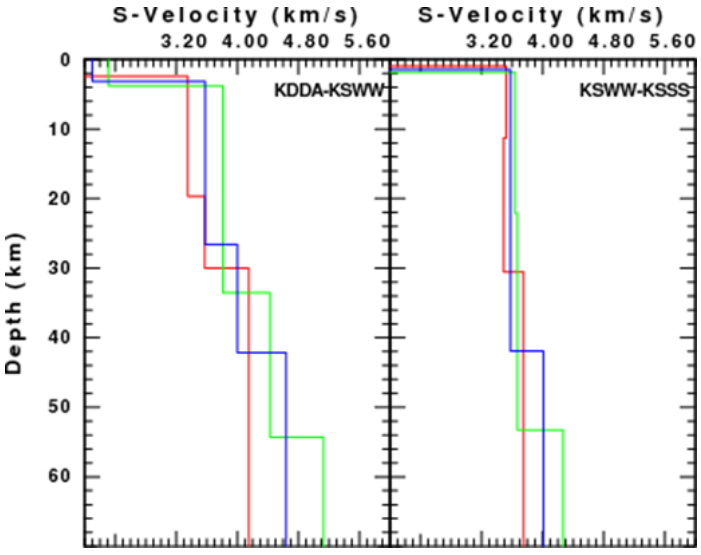

Figure-12: Comparisons between shear velocity models. Velocity models of segment KDDA-KSWW are shown to the left and those of segment KSWW-KSSS are shown to the right. In both case the best velocity model is displayed as a blue line, the lower bound velocity model is shown as a red line, and the upper bound velocity model is shown as green lines.

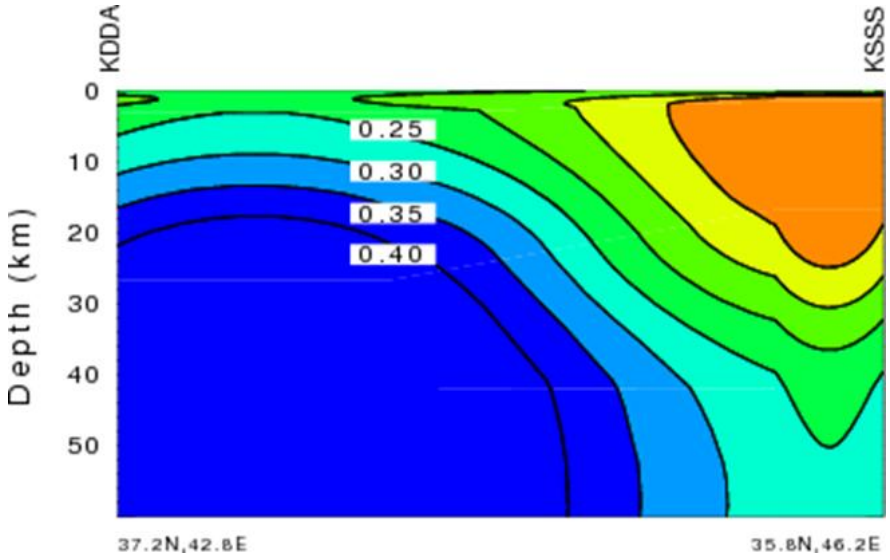

Figure-13: Shear-wave velocity standard deviation contours along the path KDDA-KSSS.

Conclusions

The application of the niching genetic algorithm (NGA) waveform inversion method to waveforms traversing the Northern Arabian Platform and surroundings has increased our understanding of this region. The NGA is used to perform regional waveform inversions for the crust and upper mantle structures. The crustal thicknesses here range from 30 to 38 km, indicating that no crustal thickening is observed in the Northern Arabian Platform or central Iran. The path that sampled the Zagros Mountains shows slower averaged velocities in comparison with the path that traversed the northern Arabian Platform.

Acknowledgments

The authors thank the Kurdistan General Directorates of Meteorology and Seismology for supporting the project. Acknowledgements are due to Mathew Sibol, Robert Wagner, Yajun Wang and Pierre Caron for analyzing and reviewing the data. Roland Gritto, Adam Sargent, Obadiah Grantland, Kevin Rogers, and David Kallus are acknowledged for installing and maintaining the stations and data centers. We are gratefull to Bakir Saeed, Borhan Salih, Aras Tawfiq, Shaho Abdullah, Ali Abdulkhaliq, Basoz Ali, Layla Omar, Nokhsha Aziz, and Nian Ahmed for helping with maintaining the stations and collecting the data. Specail thanks are due to Fadhil Khudhur, Rashid Zand, and Dara Hassan for their administrative support.

The maps in this article were created using the Generic Mapping Tools *[16]*.

References

[1] Ghalib, H. A. A., Aleqabi, G. I., Ali, B. S., Saleh, B. I., Mahmood, D. S., Gupta. I. N., Wagner, R. A. , Shore, P. J., Mahmood, A., Abdullah, S., Shaswar, O. K., Ibrahim, F., Ali, B., Omar, L., Aziz, N. I., Ahmed, N. H., Ali, A. A., Taqi, A.-K. A., and Khalaf, S. R.C.M.P. "Seismic characteristics of northern Iraq and surrounding regions," in Proceedings of the 28th Seismic Research Review: Ground-Based Nuclear Explosion Monitoring Technologies, LA-UR-06-5471, Vol. 1, pp. 40–48, 2006.

[2] Herrmann, R. B., and C. Y. Wang, A comparison of synthetic seismograms, Bull. Seism. Soc. Am., 75, no. 1, 41-56, 1985.

[3] Wang, C. Y. and Herrmann, R. B., A numerical study of P-, SV-, and SH-wave generation in a plane layered medium, Bull. Seism. Soc. Am., 70, 1015- 1036, 1980.

[4] Herrmann, R. B., Computer programs in seismology: An evolving tool for instruction and research, Seism. Res. Lett., 84, 1081-1088, doi 10.1785/0220110096, 2013.

[5] Goldberg, D. E., Genetic Algorithms in Search, Optimization and Machine Learning, Kluwer Academic Publishers, Boston, MA., 1989.

[6] Stoffa, P. L. and M.K. Sen, Nonlinear multiparameter optimization using genetic algorithms: Inversion of plane wave seismograms, Geophysics, 56(11), 1794-1810, 1991.

[7] Holland, J. H., Adaptation in Natural and Artificial Systems: An Introduction Analysis with Applications to Biology Control, and Artificial Intelligence, 183 pp., University of Michigan Press, Ann Arbor, Michigan, 1975.

[8] Mahfoud, S. W., Niching Methods for Genetic Algorithms, Ph.D. thesis, University of Illinois at Urbana-Champaign, 1995.

[9] Koper, K. D., M. E. Wysession, and D. A. Wiens, Multimodal function optimization with a niching genetic algorithm: A seismological example, Bull. Seism. Soc. Am., 89, 978-988, 1999.

[10] Aleqabi, G. I., and M. E. Wysession, Q (Lg) distribution in the Basin and Range province of the Western United States, Bull. Seism. Soc. Am., 96(1), 348-354, 2006.

[11] Robertson Maurice, S. D., D. A. Wiens, K. D. Koper, and E. Vera, Crustal and upper mantle structure of southernmost South America inferred from regional waveform inversion, J. Geophys. Res., 108 (B1), 2038, doi:10.1029/2002JB001828, 2003.

[12] Dziewonski, A. M., S. Bloch and M. Landisman, A technique for the analysis of transient seismic signals, Bull. Seism. Soc. Am., 59., 429-444, 1969.

[13] Herrin, E. E., and T. T. Goforth, Phase-Matched Filters: Application to the Study of Rayleigh Waves, Bull. Seism. Soc. Am., 67, 1259-1275, 1977.

[14] Russell, D. R., R. B. Herrmann, and H. Hwang, Application of frequency-variable filters to surface wave amplitude analysis, Bull. Seism. Soc. Am., 78, 339-354, 1988.

[15] Pasyanos, M.E., W.R. Walter, M.P. Flanagan, P. Goldstein, and J. Bhattacharyya, Building and testing an a priori geophysical model for Western Eurasia and North Africa, Pure appl. Geophys., 161, 235-281, 2004

[16] Wessel, P., and W. H. F. Smith, New, improved version of Generic Mapping Tools released, EOS Trans. Amer. Geophys. U., vol. 79 (47), pp. 579, 1998.